



# Average and local structure analysis of metastable $\text{Li}_x\text{Mn}_{0.9}\text{Ti}_{0.1}\text{O}_2$ by synchrotron X-ray and neutron sources

Naoya Ishida<sup>a,\*</sup>, Kazuki Miyazawa<sup>a</sup>, Naoto Kitamura<sup>a</sup>, Junji Akimoto<sup>b</sup>, Yasushi Idemoto<sup>a</sup>

<sup>a</sup> Faculty of Science & Technology, Tokyo University of Science, 2641 Yamazaki, Noda-shi, Chiba 278-8510, Japan

<sup>b</sup> National Institute of Advanced Industrial Science and Technology (AIST), 1-1-1 Higashi, Tsukuba-shi, Ibaraki 305-8565, Japan



## ARTICLE INFO

### Keywords:

Li-ion battery  
Cathode material  
Average structure  
Local structure  
Total scattering  
Pair distribution function

## ABSTRACT

The layered  $\text{Li}_x\text{Mn}_{0.9}\text{Ti}_{0.1}\text{O}_2$  as a cathode material for lithium-ion battery was synthesized from the precursor of  $\text{Na}_{0.7}\text{Mn}_{0.9}\text{Ti}_{0.1}\text{O}_2$  via Na/Li ion exchange. The main phase of  $\text{Li}_x\text{Mn}_{0.9}\text{Ti}_{0.1}\text{O}_2$  was identified as the layered rock-salt structure with space group  $R\bar{3}m$  using the synchrotron X-ray and neutron powder diffractions. Since the change of the charge and discharge curves of the  $\text{Li}_x\text{Mn}_{0.9}\text{Ti}_{0.1}\text{O}_2$  at the 4 V region was smaller than that of the unsubstituted material  $\text{Li}_x\text{MnO}_2$ , the transformation to spinel structure was suppressed by Ti substitution. In the PDF analysis for the synchrotron X-ray and neutron total scattering data, the structure model in which a part of Mn was located at the Li site showed better fitting than the completely ordered rock-salt structure. It was suggested that the local structure of  $\text{Li}_x\text{Mn}_{0.9}\text{Ti}_{0.1}\text{O}_2$  was characterized by the coordination environment locally similar to the spinel type in part of the layered rock-salt structure. The calculated bond-angle distortion ( $\sigma^2 = 31(2)$ ) of the  $\text{TiO}_6$  octahedra and the  $\text{MnO}_6$  octahedra ( $\sigma^2 = 39(4)$ ) from the local structure obtained by PDF analysis showed the effect of suppression derived from Ti on the distortion. Therefore, the cycle performance of  $\text{Li}_x\text{Mn}_{0.9}\text{Ti}_{0.1}\text{O}_2$  was improved by a contribution of Ti to the structural stability.

## 1. Introduction

The current lithium ion battery was realized by using  $\text{LiCoO}_2$  having a layered rock-salt type structure as a positive electrode material [1]. Since the  $\text{LiCoO}_2$  exhibits a high potential of about 4 V on the basis of Li metal and good reversibility of intercalation/deintercalation reaction with lithium, it is practically used as a positive electrode material of a lithium ion battery. Although the theoretical capacity of  $\text{LiCoO}_2$  is  $274 \text{ mAh g}^{-1}$ , the structural stability of the delithiated state becomes a problem in an actual charge-discharge reaction on delithiating about half from the  $\text{LiCoO}_2$ . The  $\text{LiCoO}_2$  contains the rare element, Co, which occupies most of the cost of the lithium ion battery. For this reason, the development of materials using Mn, Fe, etc., which are abundant in resources and inexpensive as a positive electrode material, is being pursued for considerable cost reduction.

In recent years, attention has been paid to the layered rock-salt type  $\text{LiMnO}_2$  having high theoretical capacity as a candidate for a new regulated electrode material [2–6]. Since this material contains Mn as a main component, it is less expensive and safer than Co, and has an advantage that a high capacity of  $200 \text{ mAh g}^{-1}$  or more can be obtained. However, the layered rock-salt type  $\text{LiMnO}_2$  was a metastable phase which was not synthesized by the conventional solid-state

synthesis [6–9]. The layered rock-salt type  $\text{LiMnO}_2$  underwent a phase transition to the spinel-type  $\text{LiMn}_2\text{O}_4$  during charge and discharge process and showed the low capacity retention rate. Therefore, it is necessary to synthesize a material that can suppress the transition to the spinel structure, to improve the cycle characteristic due to substitution of Ti etc. [7–9], and to demonstrate the mechanism of the substitution effect on the cycle performance. In addition, the crystal structure has not been perfectly revealed because of the existence of unknown weak peaks in the XRD patterns [7]. In average structure analysis such as Rietveld method, it is difficult to discuss the effect of substituted Ti distinctly from Mn because the major Mn and the substituted Ti occupied the same crystallographic site. Therefore, in order to evaluate the structure that cannot be explained by the average structure, we analyzed the local structure analysis, where Mn and Ti can be evaluated as individual sites by using a supercell obtained by expanding a unit cell, it is expected that the effect of Ti substitution can be clarified. To our knowledge, the research that evaluate the relationship between structure and battery characteristics from the viewpoint of the local structure have not yet been conducted on the  $\text{Na}^+/\text{Li}^+$  ion exchanged materials of the cathode materials.

In the present study, we focus on the high capacity layered rock salt-type  $\text{LiMn}_{0.9}\text{Ti}_{0.1}\text{O}_2$  with high cycle performance [7]. We attempted to

\* Corresponding author.

E-mail address: [naoya-ishida@rs.tus.ac.jp](mailto:naoya-ishida@rs.tus.ac.jp) (N. Ishida).

refine the average structure by synchrotron radiation X-ray and neutron diffraction measurements. In addition, using a refined average structure, PDF analysis using synchrotron X-ray and neutron total scattering measurements was performed to examine the local structure. The purpose of this study was to clarify the influence of Ti substitution on battery characteristics from the analyzed average and local structure.

## 2. Experimental

### 2.1. Synthesis

The  $\text{Li}_x\text{Mn}_{0.9}\text{Ti}_{0.1}\text{O}_2$  ( $x < 0.7$ ) was synthesized by the  $\text{Na}^+/\text{Li}^+$  ion-exchange for the precursor of  $\text{Na}_{0.7}\text{Mn}_{0.9}\text{Ti}_{0.1}\text{O}_2$ . The precursor was prepared by the previously reported method [7], where the  $\text{CH}_3\text{COONa}\cdot 3\text{H}_2\text{O}$  (99.8%, Wako Pure Chemical Industries, Ltd.) and Mn-Ti hydroxide were blended for 30 min at a predetermined ratio and fired at 500 °C under air at 12 h.

The precursor,  $\text{Na}_{0.7}\text{Mn}_{0.9}\text{Ti}_{0.1}\text{O}_2$ , was ion-exchanged by refluxing at 80 °C for 24 h in ethanol in which the LiBr of the 8 times molar amount of the precursors was dissolved [7,8]. After cooling to room temperature, filtration and washing with secondary distilled water, the ion-exchanged  $\text{Li}_x\text{Mn}_{0.9}\text{Ti}_{0.1}\text{O}_2$  with  $x < 0.7$  were synthesized by drying at 100 °C for 24 h.

### 2.2. Characterization and average and local structure analysis

The crystalline phases were identified with X-ray diffraction (XRD, X'pert pro, PANalytical) with  $\text{CuK}\alpha$  radiation. The measurements were scanning at 1°/min and operating at 45 kV and 40 mA with  $2\theta$  range from 10° to 70°. The lattice parameters were refined by least square method. The metal composition of the samples was determined using inductively coupled plasma (ICP) atomic emission spectroscopy (ICPE-9000, Shimadzu, Ltd.). The morphology of particle was observed with a scanning electron microscope (SEM, S-2600N, Hitachi). Each specimen was held on a conductive carbon tape and then sputtered by Au at 5 mA for 45 s. The particle diameters were detected by dynamic light scattering (FPAR-1000, Photal). The high resolution XRD data were collected by Synchrotron XRD at SPring-8 (BL19B2 beam lines). The diffracted patterns were analyzed by Rietveld method using the Rietan-FP program (Ver 2.33) [10]. The data for composite electrodes were corrected for the background using data measured by the empty capillary. In the synchrotron sources, the X-ray absorption fine structures (XAFS) were also measured at BL14B2 beam line, and the data was analyzed by the Athena program (v.0.9.21) [11].

Neutron powder diffraction measurements were taken using a time-of-flight diffractometry of iMATERIA (BL20) at the Japan-Proton Accelerator Research Complexes (J-PARC). The pulverized samples were measured about 0.2–0.4 g in the V-cell (6 mm $\phi$ ). Incident beam powers were about 150 kW at iMATERIA. The exposure time was 15 min. The structural refinements using neutron diffraction data were performed by Rietveld method using Z-Code (Version 1.0.2) [12,13].

We also performed a high-energy X-ray diffraction experiment, i.e. total scattering, with an incident beam of 61.5 keV by BL04B2 at SPring-8, Japan, and corrected the obtained data by using a standard program [14]. Neutron total scatterings were collected at NOVA (BL21), J-PARC. The synchrotron X-ray and neutron total scattering data were used within 25 Å<sup>-1</sup> and 30 Å<sup>-1</sup> in  $Q_{\text{max}}$ , respectively. The PDF analysis for total scattering data was performed by PDFgui (Release 1.0) [15].

### 2.3. Electrochemical measurement

The electrochemical cell was constructed using HS cell (Hohsen Ltd.). The cathode consisted of active material, conductive carbon and binder was applied to the synthesized active material,  $\text{Li}_x\text{Mn}_{0.9}\text{Ti}_{0.1}\text{O}_2$ , SUPER C65 (IMERYS), polytetrafluoroethylene (PTFE) with 5:5:1

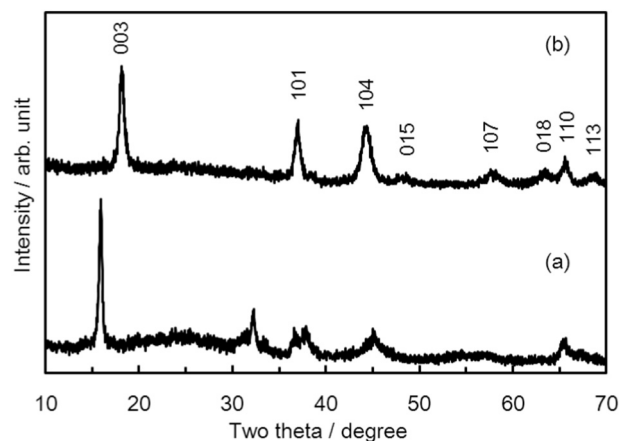


Fig. 1. Powder X-ray diffraction patterns of (a)  $\text{Na}_{0.7}\text{Mn}_{0.9}\text{Ti}_{0.1}\text{O}_2$  and (b)  $\text{Li}_x\text{Mn}_{0.9}\text{Ti}_{0.1}\text{O}_2$ .

weight ratio, respectively. The cathode was casted on the Al mesh and pressed by 20 MPa for 1 min. The anode was used as metal Li ( $\phi 15$  mm) and the electrolyte was used as 1 mol/L  $\text{LiPF}_6\text{-EC:DMC}$  (1:2 vol. ratio) and separator was used as polypropylene (Celgard #2400). These constituents were used to assemble an HS-cell in a glove-box under an argon atmosphere. A charge-discharge apparatus (HJ1010m SM8A, Hokuto Denko Corp.) was employed to conduct the charge/discharge cycle test. The charging and discharging were performed at 25 °C, the constant current of 30 mA g<sup>-1</sup> (about C/8 rate), a charge-terminating voltage of 4.8 V vs.  $\text{Li}/\text{Li}^+$  and a discharge-terminating voltage of 2.0 V vs.  $\text{Li}/\text{Li}^+$ , with a 2-min interval between the charging and discharging.

## 3. Results and discussion

### 3.1. Characterization

Fig. 1 shows the XRD patterns of the precursor,  $\text{Na}_{0.7}\text{Mn}_{0.9}\text{Ti}_{0.1}\text{O}_2$  and the ion-exchanged  $\text{Li}_x\text{Mn}_{0.9}\text{Ti}_{0.1}\text{O}_2$  ( $x < 0.7$ ). The main peaks of  $\text{Li}_x\text{Mn}_{0.9}\text{Ti}_{0.1}\text{O}_2$  were attributed to the layered rock-salt structure with  $R\bar{3}m$ . The lattice parameters obtained by the least square method were  $a = 0.2850(2)$  nm,  $c = 1.460(2)$  nm for the  $\text{Li}_x\text{Mn}_{0.9}\text{Ti}_{0.1}\text{O}_2$ . The metal compositions of the samples were measured by ICP-AES and calculated as the unity of total transition metals, Mn and Ti, contents (Table 1). The major reaction was regarded as the  $\text{Na}^+/\text{Li}^+$  ion-exchange because the transition metal compositions remained constant after the reaction. Although the  $\text{Na}^+/\text{Li}^+$  ion-exchanges were confirmed, the small amount of the residual Na and the decrease of the total alkali amounts were obtained as the same results shown in the previous works [7–9]. Thus, it involved not only the mere  $\text{Na}^+/\text{Li}^+$  ion-exchange reaction, but also the oxidation of the host materials, the detailed consideration for the valence states was described later. The morphology of the  $\text{Li}_x\text{Mn}_{0.9}\text{Ti}_{0.1}\text{O}_2$  was observed by SEM and the particle size for the sample was estimated to be about 200 nm sizes by particle-size analyzer. It does not affect the evaluation for measurements of the cathode properties due to the relatively small particles. Thus, it was considered the structural property mainly contributed to the cathode property.

Table 1

Metal compositions of the  $\text{Na}_{0.7}\text{Mn}_{0.9}\text{Ti}_{0.1}\text{O}_2$  and  $\text{Li}_x\text{Mn}_{0.9}\text{Ti}_{0.1}\text{O}_2$ . The metal compositions were calculated as the unity of sum of Mn and Ti components.

Sample	Li	Na	Mn	Ti
$\text{Na}_{0.7}\text{Mn}_{0.9}\text{Ti}_{0.1}\text{O}_2$	–	0.782 (1)	0.897 (2)	0.1022 (1)
$\text{Li}_x\text{Mn}_{0.9}\text{Ti}_{0.1}\text{O}_2$	0.594 (1)	0.0347 (1)	0.897 (4)	0.1026 (3)

Download English Version:

<https://daneshyari.com/en/article/11005953>

Download Persian Version:

<https://daneshyari.com/article/11005953>

[Daneshyari.com](https://daneshyari.com)